

GA-A25593

MAINTAINING THE QUASI-STEADY STATE CENTRAL DENSITY PROFILE IN HYBRID DISCHARGES

by

M.S. CHU, D.P. BRENNAN, V.S. CHAN, M. CHOI, R.J. JAYAKUMAR, L.L. LAO,
R. NAZIKIAN, P.A. POLITZER, H.E. ST JOHN, A.D. TURNBULL, M.A. VAN ZEELAND,
and R. WHITE

OCTOBER 2006



DISCLAIMER

This report was prepared as an account of work sponsored by an agency of the United States Government. Neither the United States Government nor any agency thereof, nor any of their employees, makes any warranty, express or implied, or assumes any legal liability or responsibility for the accuracy, completeness, or usefulness of any information, apparatus, product, or process disclosed, or represents that its use would not infringe privately owned rights. Reference herein to any specific commercial product, process, or service by trade name, trademark, manufacturer, or otherwise, does not necessarily constitute or imply its endorsement, recommendation, or favoring by the United States Government or any agency thereof. The views and opinions of authors expressed herein do not necessarily state or reflect those of the United States Government or any agency thereof.

MAINTAINING THE QUASI-STEADY STATE CENTRAL DENSITY PROFILE IN HYBRID DISCHARGES

by

M.S. CHU, D.P. BRENNAN, V.S. CHAN, M. CHOI, R.J. JAYAKUMAR,* L.L. LAO,
R. NAZIKIAN,[†] P.A. POLITZER, H.E. ST JOHN, A.D. TURNBULL, M.A. VAN ZEELAND,[‡]
and R. WHITE[†]

This is a preprint of a paper to be presented at the 21st IAEA
Fusion Energy Conference, October 16-21, 2006, in Chengdu,
China, and to be published in the *Proceedings*.

*Lawrence Livermore National Laboratory, Livermore, California.

[†]Princeton Plasma Physics Laboratory, Princeton, New Jersey.

[‡]Oak Ridge Institute for Science Education, Oak Ridge, Tennessee.

Work supported by
the U.S. Department of Energy
under DE-FG03-95ER54309, W-7405-ENG-48, DE-FC02-04ER54698,
DE-AC02-76CH03073, and DE-AC05-76OR00033

GENERAL ATOMICS PROJECT 03726
OCTOBER 2006



Maintaining the Quasi-Steady State Central Current Density Profile in Hybrid Discharges

M.S. Chu 1), D.P. Brennan 2), V.S. Chan 1), M. Choi 1), R.J. Jayakumar 3), L.L. Lao 1),
R. Nazikian 4), P.A. Politzer 1), H.E. St John 1), A.D. Turnbull 1), M.A. Van Zeeland 5), and
R. White 4)

- 1) General Atomics, P.O. Box 85608, San Diego, California 92186-5608, USA
- 2) University of Tulsa, Tulsa, Oklahoma 74104, USA
- 3) Lawrence Livermore National Laboratory, Livermore, California 94550, USA
- 4) Princeton Plasma Physics Laboratory, Princeton, New Jersey 08543, USA
- 5) Oak Ridge Institute for Science Education, Oak Ridge, Tennessee 37831, USA

e-mail contact of main author: chum@fusion.gat.com

Abstract. Experimental observations in tokamaks operated in hybrid regime revealed that the presence of a rotating neoclassical island substantially reduce the occurrence of sawteeth. Three mechanisms relevant to the possibility of a rotating magnetic island driving counter currents in tokamaks are investigated, with two mechanisms driving sufficient current to prevent sawteeth. They rely on establishing a parallel electric field by the rotating neoclassical island. First is the excitation of an electrostatic side band through diamagnetic and curvature drifts; second is excitation of the kinetic Alfvén wave through the polarization drifts. The third mechanism is modification of energetic particle distribution function by the neoclassical island, which is found to be relatively weak.

1. Introduction

The hybrid discharge scenario is an attractive operating regime for ITER operation. It can operate near the $n=1$ stability limit with good confinement and maintain near steady state. The projected ITER performance is at or above $Q_{\text{fusion}} = 10$. It is projected to be compatible with sustained ignition in ITER. This discharge scenario has been observed in many devices, i.e., DIII-D [1-3], JET [4], ASDEX-U [5], and JT-60U [6]. It is important to maintain the current profile at steady state. One desirable goal could be the elimination of the sawtooth. In experiments in DIII-D and worldwide, an intriguing correlation of the existence of a neoclassical island with reduced activity of sawtooth has been found. The magnetic island does not adversely affect plasma confinement, yet it is correlated with the reduction of the sawteeth oscillation. Apparently, the rotating neoclassical island provides a mechanism for negative current drive near the plasma center which prevents further drop of the central q_0 below 1 that would ordinarily trigger sawteeth.

This conjecture is verified in a careful accounting of the current components during a hybrid discharge with a rotating island. The predicted driven currents according to transport analysis are compared with observed fitted current profile and shown in Fig. 1 [3]. The total amount of negative current (in red) is ~ 50 (kA) and is about 5% of plasma current and localized inside the island radius. The amount of negative current, although small, is what is needed to make $q_0 \geq 1$. The purpose of this work is to explore the physical processes due to the rotating magnetic island which contributed to the negative current drive.

A rotating magnetic island can be viewed as an antenna embedded in the plasma. It emits Alfvén waves in the plasma at the rotation frequency of the island. The general theory of Fisch and Karney [7] pointed out that for current drive, it is crucial to determine the parallel electric field. The perpendicular electric field is readily deduced from observations and the

MHD equations. The parallel electric field is zero in the MHD approximation and must be determined from kinetic theories. We followed Rosenbluth and Rutherford [8] to derive the general relationship between the parallel and perpendicular electric fields in a rotating plasma. Kinetic theory determines the parallel electric field resulting from the polarization, magnetic and diamagnetic drifts resulting in two different kinds of parallel electric fields.

Our results are: first, the rotating neoclassical island can drive side band parallel electric fields through charge separation due to magnetic curvature drift which can drive substantial counter current that prevented the occurrence of sawtooth. The driven current is predominantly carried by the lower sideband. It is particularly large when the central q_0 value is near 1 and the q profile is flat. Second, the parallel electric field driven by polarization drift is usually negligible. However, when this charge separation results in the excitation of the kinetic Alfvén wave (KAW) [9] then the driven current can still be appreciable. The KAW can be viewed as a set of normal modes that are excited by the rotating neoclassical islands. Similar to curvature drift, this process requires a rotating island, with central q_0 value very close to 1 and the q profile being flat!

Third, in tokamaks, substantial amount of current is driven by the NBI injected energetic ions. NBI driven current can be reduced if the energetic particle distribution function can be broadened by the neoclassical island. We studied this process using the ORBIT code [10] to follow the redistribution of the ions by the rotating magnetic island. We did not find any additional resonance of the energetic particles with the magnetic perturbations. The energetic ions very quickly come to equilibrium with the perturbed magnetic field with its density distribution slightly broadened. This process cannot account for all the observed counter currents.

2. General Relations for Currents Driven by an MHD Wave

A rotating magnetic island can be viewed as an antenna embedded inside the plasma which emits MHD (Alfvén) waves to the surrounding plasma. Fisch and Karney [7] have provided a quasilinear theory for computing the current driven by waves in general. The driven current density J is directly proportional to the dissipated power density P_d by the universal formula

$$\frac{J/en_0v_{Te}}{P_d/m_en_0v_e v_{Te}^2} = \frac{8}{\omega_a} + 2 + 1.4\omega_a^2 \quad . \quad (1)$$

In Eq. (1), n_0 is the plasma density, $\omega_a = (\omega_{Is}^e)/k_{\parallel}v_{Te}$ is the phase velocity of the wave relative to the electron thermal speed in the frame of the electron fluid. v_e is the electron-ion collision frequency. The dissipated power density is given by $P_d = -m_en_e \int v_{\parallel} D_{rf} (\partial f / \partial v_{\parallel}) d\bar{v}$. The quasi-linear diffusion operator is given by $D_{rf} = (\pi e^2 \langle E_{\parallel}^2 \rangle) / m_e^2 v_{\parallel 0} \Delta k$ with $v_{\parallel 0}$ being the

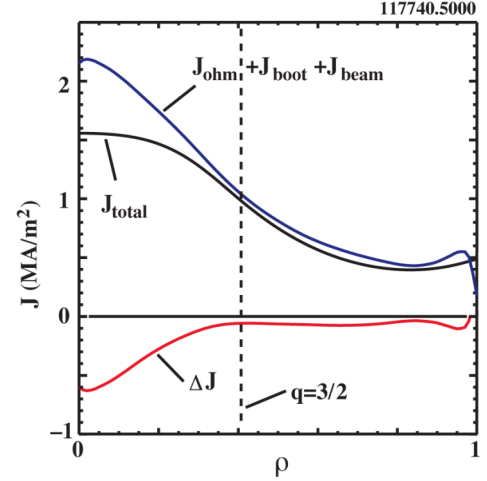


FIG. 1. Current density deficit (colored curve) in a hybrid DIII-D discharge shot 117740. The J_{total} is obtained from the EFIT equilibrium code. The expected driven current is from transport code analysis which predicted currents from Ohmic, bootstrap and beam drive and shown in $J_{ohm} + J_{boot} + J_{beam}$.

parallel velocity of the resonant electrons and Δk being the spread in wave number of the oscillating external wave. For a Maxwellian electron distribution

$$P_d = \frac{n_0 \pi e^2 \langle E_{\parallel}^2 \rangle}{\sqrt{2\pi} m_e v_{Te}^3} \exp \left[-\frac{(\omega_{Is}^e)^2}{2v_{Te}^2 k_{\parallel}^2} \right] \frac{(\omega_{Is}^e)^2}{k_{\parallel}^3} . \quad (2)$$

Quantities in Eq. (2) are readily obtained from experimental measurements, except E_{\parallel} . We have to relate it to the observed MHD oscillation associated with the neoclassical island.

In MHD, E_{\perp} is easily obtained. The perturbed magnetic field $\delta \vec{B}$ is related to plasma displacement $\vec{\xi}$ through $\delta \vec{B} = \vec{\nabla} \times (\vec{\xi} \times \vec{B}_0)$. Here \vec{B}_0 is the equilibrium magnetic field. $\vec{\xi}$ may be regarded as known for instance from ECE emissions. In this work, we also assume the electric field may be represented as $\vec{E} = -\vec{\nabla}_{\perp} \phi - \vec{\nabla}_{\parallel} \psi$ or $\vec{E}_{\parallel} = -\vec{\nabla} \psi$. For a m/n island with (poloidal, toroidal) mode number $(m=n+1, n)$, rotating with a constant velocity ω_{Is} relative to the plasma, (tacitly assuming $m/n=3/2$, easily generalized to different m/n values) we can obtain ϕ from the perpendicular component of the induction equation,

$$\phi = \frac{\omega_{Is}^i B_0 \xi_{\psi}}{k_{\perp}} . \quad (3)$$

k_{\parallel} , and k_{\perp} are the (parallel, perpendicular) wave numbers. The fluctuating potential given in Eq. (3) generates charge separation through the polarization, magnetic and diamagnetic drifts, resulting in charges that reflect the mode structure of the perturbation ϕ . The electrons and ions will move along the field line to reduce these charge accumulation. For a given perpendicular electric field, the parallel electric field is determined by the charge neutrality condition. Because particle motion along the field line and the drifts across the field line depends on the field line geometry, this charge neutrality condition has an important implicit dependence on the field line geometry. In particular, these drifts may result in an enhanced response to ϕ and this gives rise to the excitation of new modes (the KAW) in the system.

Using the drift kinetic equation, we generalized Rosenbluth's and Rutherford's [8] derivation of the response of the distribution function to the perturbed potential. The diamagnetic effects and plasma rotation were included. For the ions we obtain

$$\frac{T_i \tilde{n}_i}{n_0 |e|} = -\frac{\bar{\omega}_i^*}{\omega_{Is}^i} \phi - \frac{Z(\zeta_0^i)}{\sqrt{2} k_{\parallel} v_{Ti}} \left(\omega_{Is}^i \rho_i^2 \nabla_{\perp}^2 + \langle \bar{\omega}_D^i \rangle \right) \left(1 - \frac{\bar{\omega}_i^*}{\omega_{Is}^i} \right) \phi - \left[1 + \zeta_0^i Z(\zeta_0^i) \right] \left(1 - \frac{\bar{\omega}_i^*}{\omega_{Is}^i} \right) \psi . \quad (4)$$

where $\zeta_0^i = (\omega_{Is}^i) / (\sqrt{2} k_{\parallel} v_{Ti})$, ρ_i is ion Larmor radius, $\langle \rangle$ average over velocity space, and plasma dispersion function $Z(\zeta) = (1/\sqrt{\pi}) \int_{-\infty}^{\infty} \exp(-\beta^2) d\beta / (\beta - \zeta)$. In Eq. (4), the potentials ϕ and ψ are spatially dependent functions. The diamagnetic drift $\bar{\omega}_i^* = (iT_i/B|e|l_{\psi}) (\vec{b} \times \hat{\psi} \cdot \nabla)$, with l_{ψ} being the density scale length, \vec{b} the unit vector of the unperturbed magnetic field, $\hat{\psi}$ the unit vector normal to the flux surface; and $\omega_D^i = -i [m_i (\mathbf{u}B + v_{\parallel}^2) / |e|B^2] \vec{b} \times \nabla B \cdot \nabla$ are operators on perturbed potentials. There is also a non-negligible current carried in the central

plasma region, we note that the wave is moving at a different frequency, ω_{Is}^e , relative to the electrons. It is easy to write down the corresponding density perturbation for the electrons. After canceling out the charges from the ω^* term (direct ExB motion), the charge neutrality condition is easily written as

$$\sum_s \frac{T_e}{T_s} \left[1 + \zeta_s Z(\zeta_s^0) \right] \left(1 - \frac{\bar{\omega}_s^*}{\omega_{\text{Is}}^i} \right) \psi = - \sum_s \frac{Z(\zeta_s^0) T_e}{T_s \sqrt{2} v_{\text{ts}} k_{\parallel}} \left(\omega_{\text{Is}}^i \rho_s^2 \nabla^2 + \langle \bar{\omega}_{\text{D}}^i \rangle \right) \left(1 - \frac{\bar{\omega}_s^*}{\omega_{\text{Is}}^i} \right) \phi \quad (5)$$

Here, ζ_s includes the modification to ζ_s^0 due to parallel velocity. We emphasize again that Eq. (5) is for general spatial dependence for both ϕ and ψ and the drifts should be treated as operators. We specialize to the limit in which the wave phase speed is much less than the electron thermal speed. The operator operating on ϕ in Eq. (5) is dominated by the contribution from the ions. If we also assume that the wave speed is faster than the ion thermal speed, the operator operating on ψ is dominated by the electrons. In this (drift wave) limit, which is expected to be the most important frequency regime, we may formally solve for ψ in terms of ϕ

$$\psi = - \left\{ \left[1 + \zeta_e Z(\zeta_e^0) \right] \left(1 - \frac{\bar{\omega}_e^*}{\omega_{\text{Is}}^i} \right) \right\}^{-1} \frac{T_e}{T_i} \left(\rho_i^2 \nabla^2 + \frac{\langle \bar{\omega}_{\text{D}}^i \rangle}{\omega_{\text{Is}}^i} \right) \left(1 - \frac{\bar{\omega}_s^*}{\omega_{\text{Is}}^i} \right) \phi \quad (6)$$

Substitution of Eq. (2) into Eq. (1), and using Eq. (6) to express the parallel electric potential ψ in terms of the perturbation potential ϕ , and further use Eq. (3) to express ϕ in terms of the plasma displacement, we can obtain an expression for the driven current density J .

$$J = J_{\text{MHD}} f_{\perp} f_{\parallel} \quad , \quad J_{\text{MHD}} = \frac{\sqrt{2\pi^3} \epsilon_0^2 \omega_{\text{Is}}^e (\omega_{\text{Is}}^i)^2 B^2 \xi_{\psi}^2}{e \ln \Lambda k_{\perp}^2} \quad , \quad (7)$$

$$f_{\perp 1} = \left[\frac{T_e}{T_i} k_{\perp}^2 \rho_i^2 \left(1 - \frac{\omega_i^*}{\omega_{\text{Is}}} \right) \right]^2 \quad , \quad f_{\perp 2} = \left[\frac{T_e \langle \bar{\omega}_{\text{D}}^i \rangle}{T_i \omega_{\text{Is}}^i} \left(1 - \frac{\omega_i^*}{\omega_{\text{Is}}} \right) \right]^2 \quad , \quad (8)$$

$$f_{\parallel} = \left[1 + \frac{\omega_a}{\sqrt{2}} Z\left(\frac{\omega_a}{\sqrt{2}}\right) \left(1 - \frac{\omega_e^*}{\omega_{\text{Is}}} \right) \right]^{-2} \exp\left(-\frac{\omega_a^2}{2}\right) (8 + 2\omega_a + 1.4\omega_a^2) \quad . \quad (9)$$

In the above formulae, the f_{\perp} factors are determined by ion dynamics; the f_{\parallel} factor determined by electron dynamics. We separated the f_{\perp} into two terms, since these are from different origins. $f_{\perp 1}$ has its origin from polarization drift and is diagonal with respect to the poloidal mode number; whereas $f_{\perp 2}$ has its origin from magnetic curvature drift and is off diagonal with respect to the poloidal mode number. The effect of these terms can only be added after they are squared. Although the form of f_{\parallel} is the same, but the proper poloidal mode number should be used in its evaluation together with the f_{\perp} term. It is interesting to note that as a function of ω_a , the variation of f_{\parallel} is very simple, as shown in Fig. 2 (after ignoring first the small ω_e^* factor). It is seen that f_{\parallel} ranges between 8 and 18, for ω_a varying between 0 to 3.5.

Beyond $\omega_a = 4$, this factor is essentially 0. Due to the factor $(k_{\perp}^2 \rho_i^2)^2$, $f_{\perp 1}$ is very small $\sim 10^{-4}$ making the amount of current driven negligible. $f_{\perp 2}$ is also small, but it scales as $(\rho_i/R)^2$, therefore, is larger than $f_{\perp 1}$. $f_{\perp 1}$ can only become large through mode conversion when k_{\perp} changes.

3. Current Drive Through Magnetic Curvature Drift Induced Charge Separation

In tokamaks, $|B|$ is non-uniform. The magnetic curvature drift is parallel to the axis of symmetry. For a magnetic island with poloidal and toroidal mode number m/n , charge separation due to magnetic curvature drift has mode numbers $(m+1)/n$ or $(m-1)/n$. In the limit of circular tokamaks with $\phi(\vec{r})$ given by $\phi(r)\exp(in\zeta - im\theta)$, the upper and lower sidebands of the perturbed parallel potentials shown in Eq. (5) are given by

$$\psi_{\pm} = i \frac{\sum_s \frac{1}{e_s B R} \left(1 - \frac{\omega_s^*}{\omega_{Is}^i}\right) \frac{1}{\sqrt{2} v_{ts} k_{\parallel \pm}} Z(\zeta_{s\pm}) \left(\frac{m+1}{r} \phi \mp \frac{\partial \phi}{\partial r}\right)}{\sum_s \frac{1}{T_s} \left[1 + \zeta_{\pm} Z(\zeta_{\pm}^0)\right] \left(1 - \frac{\omega_{s\pm}^*}{\omega_{Is}^i}\right)} \quad (10)$$

To further elucidate the nature of this curvature-drift sideband coupling current drive process and to obtain a realistic estimate of the total amount of driven current, we evaluated Eqn (7) through (9), using Eq. (10) for ψ for a large aspect ratio circular tokamak with parameters relevant to DIII-D. More specifically, we took DIII-D parameters with $B = 1.75$ T, $T_e = 4$ keV, $T_i = 7$ keV, $\omega_{Is}^i = 1.5 \times 10^4$ s, $\omega_{Is}^e = 4.5 \times 10^4$ s, $\ln \Lambda = 10$, $\omega_A = 3 \times 10^6$ /s, $\rho_i = 4 \times 10^{-3}$ m, $r_{Is} = 0.3$ m, $f_{\parallel} = 15$. The q profile is assumed to be given by $q = q_0 + (1.5 - q_0)(r/r_s)^{\alpha_q}$. The results are shown in Fig. 3. The neoclassical island is assumed to be a $m/n = 3/2$ island, with an amplitude half width of 3 cm. It is seen that a substantial amount of current can be driven by this process. Most of the current comes from the lower sideband. When the q_0 value gets close to 1, the parallel wave vector can become small and it becomes very efficient in driving the current. When q_0 becomes sufficiently close to 1 and the q profile is sufficiently flat, with $\alpha_q \sim 3$,

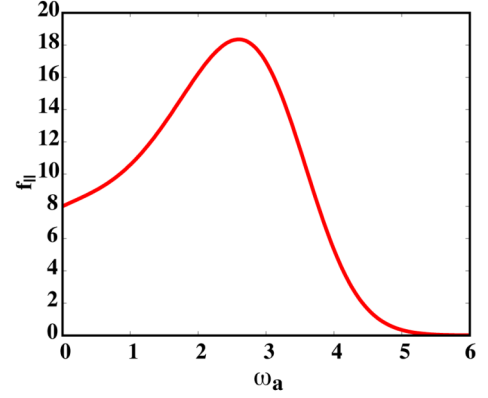


FIG. 2. Variation of f_{\parallel} as a function of ω_a – the phase velocity of the wave relative to the electron thermal speed.

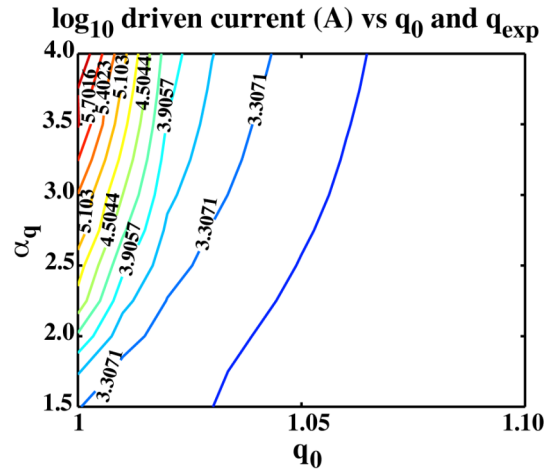


FIG. 3. Amount of counter current driven by a rotating neoclassical $3/2$ island through induced charge separation due to magnetic curvature drift plotted as a function of the central q_0 value and the flatness of the q profile. The parameters chosen are appropriate for DIII-D. The driven current is mostly due to the lower $(2/2)$ sideband electric field.

the driven current can be up to 50 kA (note the green curve marked 4.5 for the logarithm of the total driven current in Amperes). It is expected that a slightly hollow q profile, with $q_{\min} \sim 1$ located slightly off axis would result in more driven counter current.

4. Current Drive Through Excitation of Kinetic Alfvén Waves

The KAW is a plasma wave excited by the Alfvén wave through mode conversion at the Alfvén resonance. Contrary to previous works utilizing externally generated Alfvén waves by an antenna, in this study we focus on Alfvén waves generated by the rotating magnetic island and its rotation relative to the background plasma [11]. We kept terms up to 4th order in the ion Larmor radius. The resultant equation can be written in the following form:

$$\rho_i^2 \left[\frac{T_e}{T_i} \frac{\left(1 - \frac{\omega_s^*}{\omega_{Is}^i}\right)}{\left(1 - \frac{\omega_e^*}{\omega_{Is}^i}\right)(1 + i\sqrt{\pi}\zeta_e)} + \frac{3}{4} \omega_{Is}^i (\omega_{Is}^i - \omega_i^*) \right] \nabla^4 \phi - \bar{\nabla} \cdot \left[k_{\parallel}^2 v_A^2 - \omega_{Is}^i (\omega_{Is}^i - \omega_i^*) \right] \bar{\nabla} \phi + \dots = 0 \quad (11)$$

Only terms affecting the structure of the Alfvén wave and the KAW are shown. The $\nabla^4 \phi$ term is usually $\rho_i^2 k_{\perp}^2$ smaller than the 2nd order derivative term and negligible. Near the resonance of the Alfvén wave given by $\omega_{Is}^i (\omega_{Is}^i - \omega_i^*) - k_{\parallel}^2 v_A^2 = 0$, the $\nabla^4 \phi$ term facilitates mode conversion. The scale length becomes $L = \left(\rho_i^2 \left[(T_e/T_i) + 3/4 \right] (\omega_{Is}^i / 2n\omega_A) (dr/dq) \right)^{1/3}$. Then the $f_{\perp 1}$ factor in Eq. (8) is modified to

$$f_{\perp 1} = A^2 \left(\frac{T_e}{T_i} \right)^2 \left[\frac{\rho \frac{dq}{dr}}{\left(\frac{T_e}{T_i} + \frac{3}{4} \right) \frac{\omega_{Is}^i}{2n\omega_A}} \right]^{4/3} \left(1 - \frac{\omega_i^*}{\omega_{Is}^i} \right)^2. \quad (12)$$

A is an amplification factor resulting from mode conversion. Equations (7), (8), (9), and (12), give the expected KAW current density driven by the m/n island after mode conversion. Integration of the current density given in Eq. (7), then gives the total amount of current driven by mode conversion. We also solved Eq. (11), with the inclusion of the diamagnetic effects and the kinetic damping terms and with parameters appropriate for the DIII-D discharges as given in the previous section. The factor A has been found to be very sensitive to the q profile. Shown in Fig. 4 is the total amount of driven current as a function of a_q for $q_0 = 1.002$. The (dotted, solid) lines are results (with, without)

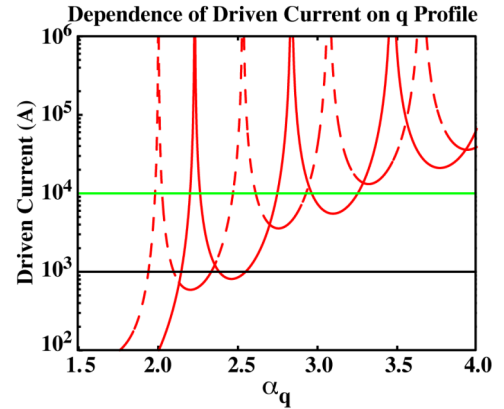


FIG. 4. Numerical computed driven current as a function for equilibria with $q_0 = 1.002$ and q profile parameter a_q . Solid lines do not include the kinetic terms, dotted lines do. It is seen that the total driven current depends sensitively on the q profile. The reason being that the Alfvén wave and KAWs developed a resonant cavity mode in the region inside of the $q = 3/2$ surface.

the diamagnetic and damping terms. It is seen that the structure of the parameter space is basically not determined by the kinetic terms, manifesting a set of eigenmodes in the system. We also see that there are parameter regions with substantial amount of driven current up to 10^4 to 10^5 A. Since the parameter range for large amount of driven current is narrow, we expect these current drive processes to be intermittent. Shown in Fig. 5 is the variation of total amount of driven current as a function of q_0 and also α_q . The large current drive region in the parameter space is clearly connected and showing the resonant nature of the process. Within these strong current drive regions, the plasma becomes a *resonant* cavity for the system of AW-KAWs. Even a relatively small amplitude of 2/2 component at the 3/2 surface will give rise to a substantial driven current. We note that the predicted amount of driven current could modify the q profile and could be experimentally observable [12].

5. The Effect on the Energetic Particle Distribution Function

The neoclassical island and its associated side band oscillations is also expected to affect the behavior of energetic particles which could in turn also affect the current drive process. This effect is studied using the Hamiltonian guiding center particle code ORBIT. The magnetic geometry used is the DIII-D equilibrium with magnetic perturbation as described in the previous sections. The resultant magnetic field line structure is shown in the Poincare plot Fig. 6. The 3/2 island structure is clearly visible with minimal stochasticity. The study followed the particle trajectory of up to 2 million particles. Starting with an initial particle distribution within the unperturbed 3/2 surface, the resultant particle density is recorded after the new distribution has reached a “steady state”. It is found that the energetic particles reached a new steady state after just completing a few toroidal turns in their orbit. The deviation from the initial state is proportional to the amplitude of the MHD perturbation. Also, this deviation is relatively independent of the energy of the energetic particles. The resultant density profiles of the energetic particles are shown in Fig. 7 as a function of the assumed MHD perturbation amplitude. All these are consistent with the assumption that the energetic particles established a new distribution that follow the perturbed helical MHD equilibrium. No additional anomalous scattering by the

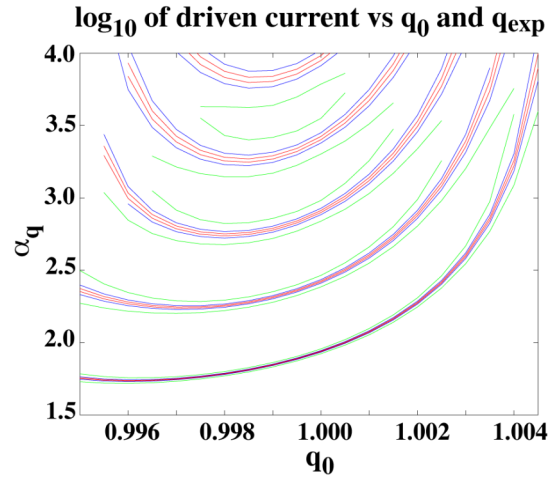


FIG. 5. Numerical computed total driven current as a function for equilibria with q_0 and q profile parameter α_q . The (green, blue, red) curves bound regions with total driven current larger than (1, 10, 100) kA. These regions are connected showing the trajectory of the resonant mode.

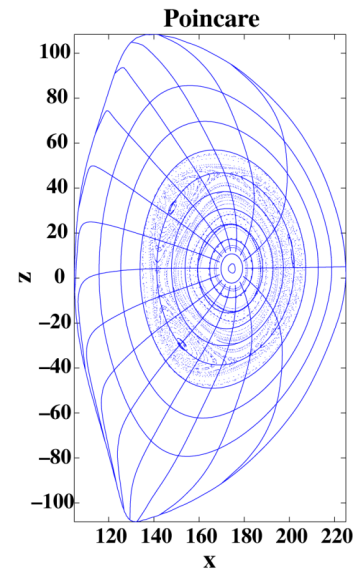


FIG. 6. Plasma geometry and Poincare plot of magnetic field line structure used in the study of effect of magnetic perturbation of the 3/2 island on the distribution of energetic particles. The magnetic island is clearly visible with minimal field line stochasticity.

MHD perturbations need be invoked. From ECE emission and from external Mirnov probes, we may infer that the full island size is less than 10 cm. A simple calculation based on the total area in which the energetic ions has to be spread out gives the reduction of the energetic ion density within the unperturbed 3/2 region to be ($A_{\text{island}}/A_{\text{Is}} = 2\Delta r/r_{\text{Is}}$). This needs to be multiplied by a profile factor and also a fraction of the neutral beam current drive factor. This gives $\sim 10\%$ - 20% of the missing current. We conclude that although this process contributes to the missing current, this alone is not sufficient to account for the full missing current.

6. Conclusion

The motivation of the present work is the observation that in a number of tokamaks operated in the hybrid regime, the presence of a rotating neoclassical island substantially reduces the occurrence of sawteeth. This indicates that the rotating island is driving counter current at the plasma center. The physical processes that lead to this counter current drive in present day rotating tokamaks is investigated. Three mechanisms that contributed to this counter current drive were investigated. Two of them have been found sufficient to drive the missing current transiently. These processes rely on establishing a parallel electric field by the rotating neoclassical island. First is the excitation of an electrostatic side band through diamagnetic and curvature drifts. Second is excitation of the kinetic Alfvén wave at the plasma center through the polarization drifts. The third mechanism is modification of the energetic particle distribution function by the neoclassical island and has been found to be relatively weak and not sufficient to account for the total missing current. Lastly, these processes are studied in the context of MHD waves in general. They can be utilized in ITER for the stabilization of sawtooth.

This work was supported by the U.S. DOE under DE-FG03-95ER54309, DE-FC02-04ER54698, W-7405-ENG-48, DE-AC02-76CH03073, and DE-AC05-76OR00033. The author acknowledges discussions with Drs. L. Chen, Q.D. Gao, F.W. Perkins, A. Wang, and K.L. Wong.

References

- [1] LUCE, T.C., *et al.*, Nucl. Fusion **43** (2003)321.
- [2] WADE, M.R., *et al.*, Nucl. Fusion **45** (2005) 407.
- [3] POLITZER, P.A., *et al.*, Proc. 32nd EPS Conf. on Plasma Physics, Terragona, Spain (2005) Paper 01.001
- [4] JOFFRIN, E., *et al.*, Nucl. Fusion **45** (2005) 626.
- [5] SIPS, A.C.C., *et al.*, Plasma Phys. Control. Fusion **44** (2002) B69.
- [6] ISAYAMA, A., *et al.*, Nucl. Fusion **43** (2003) 1272.
- [7] FISCH, N.J., and KARNEY, C.F.F., Phys. Fluids **24** (1981) 27.
- [8] ROSENBLUTH, M.N., and RUTHERFORD, P.H., Phys. Rev. Lett. **34** (1975) 1428.
- [9] HASEGAWA, A., and CHEN, L., Phys. Rev. Lett. **32** (1974) 454.
- [10] WHITE, R., *The Theory of Toroidally Confined Plasmas*, Rev. 2nd Ed., Imperial College Press, London (2006).
- [11] CHU, M.S., *et al.*, "Kinetic Alfvén Waves and Associated Current Drive at Center of Tokamaks," to be published in Phys. Plasmas (2006).
- [12] VANZEELAND, M.A., and NAZIKIAN, R., private communication (2006).

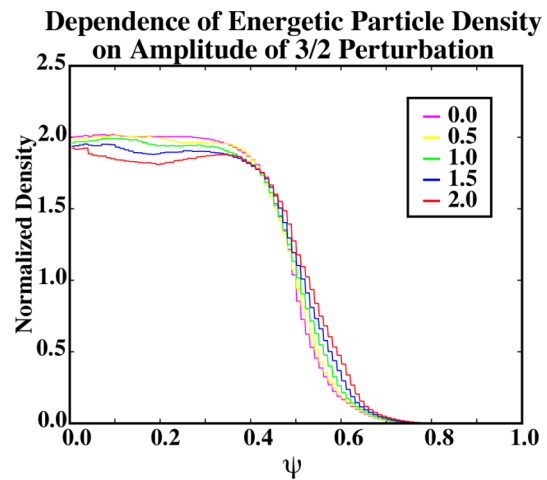


FIG. 7. Density redistribution of the energetic particles due to the rotating central neoclassical island. The deviation from the original distribution is proportional to the amplitude of the perturbation.